

Coulomb-enhanced dynamic localization and Bell state generation in coupled quantum dots

Ping Zhang^{1,2}, Qi-Kun Xue¹, Xian-Geng Zhao², X.C. Xie^{3,1}

¹*International Center of Quantum Structure and State Key
laboratory for*

*Surface Physics, Institute of Physics, The Chinese Academy of Sciences,
Beijing 100080, P.R. China*

²*Institute of Applied Physics and Computational Mathematics, Beijing
100080, P.R. China*

³*Department of Physics, Oklahoma State University, Stillwater, OK 74078*

Abstract

We investigate the dynamics of two interacting electrons in coupled quantum dots driven by an AC field. We find that the two electrons can be trapped in one of the dots by the AC field, in spite of the strong Coulomb repulsion. In particular, we find that the interaction may enhance the localization effect. We also demonstrate the field excitation procedure to generate the maximally entangled Bell states. The generation time is determined by both analytic and numerical solutions of the time dependent Schrödinger equation.

PACS numbers: 03.65.Ud, 78.67.Hc, 73.23.-b

Keywords: coupled quantum dots, dynamical localization, entanglement

I. INTRODUCTION

Quantum-state engineering via optical or electrical manipulation over the coherent dynamics of suitable quantum-mechanical systems has become a fascinating prospect of modern

physics. A very intriguing result in the study of a single particle in a double-trap system exposed to a time-dependent external field is the dynamic localization phenomenon [1,2,3], i.e., for appropriate field parameters, a localized wave packet remains dynamically localized during the subsequent time evolution. This driving induced trapping has been theoretically and experimentally studied in many physical and chemical systems [4,5,6].

When two or more interacting particles are present, apart from the highly nontrivial question of whether the strong many-body interaction can be overcome for the particles to create and preserve localization, the possibility of entanglement of the many-body wave functions arises. Entanglement is an essential ingredient in any scheme of quantum information processing. Recently, quantum dot realizations of the entanglement have received increasing attention. Various schemes based on electron spins and electron-hole pairs have been proposed to implement quantum computer hardware architectures [7,8,9,10,11]. Although there have been some numerical studies on interacting electron systems driven by an AC field [12,13,14], there is still little theoretical understanding of the observed effects beyond the phenomenology level at the present time.

In this paper, we address the dynamic localization and quantum entanglement of two interacting electrons in a double quantum dot system driven by an AC field (see Fig. 1). We show that with certain choice of parameters, in contrast to direct intuition, the Coulomb repulsion may enhance the localization due to the level crossing associated with different symmetries of a dynamic parity operation (discussed in more detail later). We also show that the maximally entangled Bell state can be prepared and maintained with a pulse of an AC field. Our study provides useful information for the future exploitation of coherent control of two-electron states in quantum dots.

In Sec. II we present the Hamiltonian for two interacting electrons in a double-dot system. A simplified spin-1 representation of the Hamiltonian is given in Sec. III. In Sec. IV we discuss the phenomenon of Coulomb-enhanced localization. The field excitation procedure to generate the maximally entangled Bell state is showed in Sec. V. A summary is given in Sec. VI.

II. THEORETICAL MODEL

The Hamiltonian which we use to describe the dynamics of two interacting electrons in a coupled quantum dot driven by electric field is

$$H(t) = \sum_{i=1,2} h(\mathbf{r}_i, \mathbf{p}_i, t) + V_C(|\mathbf{r}_1 - \mathbf{r}_2|), \quad (1a)$$

$$h(\mathbf{r}, \mathbf{p}, t) = \frac{\mathbf{p}^2}{2m^*} - ezF(t) + V_t(\mathbf{r}) + V_l(\mathbf{r}), \quad (1b)$$

$$V_C(|\mathbf{r}_1 - \mathbf{r}_2|) = \frac{e^2}{\kappa|\mathbf{r}_1 - \mathbf{r}_2|}, \quad (1c)$$

where $V_C(|\mathbf{r}_1 - \mathbf{r}_2|)$ is the Coulomb interaction and h the single-particle Hamiltonian. The time-dependent electric field $F(t)$ is applied along the inter-dot axis. The dielectric constant κ and the effective mass m^* are material parameters. The potential V_t in h describes the in-plane confinement, whereas V_l models the longitudinal double-well structure. The transverse coupling of the dots is modeled by a harmonic potential

$$V_t(x, y) = \frac{m^*\omega_t^2}{2}(x^2 + y^2). \quad (2)$$

It has been shown in experiments with electrically gated quantum dots in a two-dimensional electron system that the electronic spectrum is well described by a simple harmonic oscillator [15]. In describing the confinement V_l along the inter-dot axis, we use a (locally harmonic) double well potential of the form

$$V_l = \frac{m^*\omega_l^2}{8a^2}(z^2 - a^2)^2, \quad (3)$$

which, in the limit of large inter-dot distance, separates into two harmonic wells (one for each dot) of frequency ω_l . Although in principle a square-well potential would be a more accurate description of the real potential than the harmonic double well, there is no qualitative difference between the results presented below obtained with harmonic potential and the corresponding results using square-well potential.

We assume the transverse confinement is strong enough. Thus, the (x, y) degrees of freedom are frozen in the dynamics and the two-electron wave function can be written as $|\Psi(\mathbf{r}_1, \mathbf{r}_2, t)\rangle = |\phi(x_1, y_1)\rangle|\phi(x_2, y_2)\rangle|\Phi(z_1, z_2, t)\rangle$, where $|\phi(x, y)\rangle$ is the transverse ground state. Considering the fact that the external electric field is applied along the longitudinal direction, the approximation of frozen in-plane motion is reasonable and has been employed in previous work [13]. After integrating over the (x, y) degrees of freedom, the time dependent Schrödinger equation becomes

$$i\hbar\frac{\partial|\Phi(z_1, z_2, t)\rangle}{\partial t} = \left[-\frac{\hbar^2}{2m^*}\left(\frac{\partial^2}{\partial z_1^2} + \frac{\partial^2}{\partial z_2^2}\right) + V(z_1) + V(z_2) + V_C(|z_1 - z_2|) - eF(t)(z_1 + z_2)\right]|\Phi(z_1, z_2, t)\rangle, \quad (4)$$

where V_C is the effective one-dimensional Coulomb interaction

$$V_C(|z_1 - z_2|) = \int dx_1 dx_2 dy_1 dy_2 \frac{e^2 \phi^2(x_1, y_1) \phi^2(x_2, y_2)}{\kappa |\mathbf{r}_1 - \mathbf{r}_2|}. \quad (5)$$

We use the effective mass m^* and dielectric constant κ of GaAs. The other parameters are chosen as $\hbar\omega_l = 20\text{meV}$ and $a = 20\text{nm}$.

The time evolution of the two electrons is obtained by numerically solving the Schrödinger equation (4) using an extension of the Crank-Nicholson method [16] to two spatial dimensions. The initial state used in this investigation is the field-free ground state, which is obtained by propagating a trial two-particle wave packet in the imaginary time domain and shown in Fig. 2(a). As illustrated by the spatial symmetry under the particle exchange, the ground state is a singlet, as expected. Since Eq. (4) contains no mixing between the singlet and triplet sub-spaces, the dynamics of the system will always be confined to the singlet sub-space.

III. SPIN-1 REPRESENTATION OF THE HAMILTONIAN

To understand the underlying physics behind the numerical results we employ the Hund-Mulliken (HM) approximation by introducing the orthonormalized one-particle wave

functions $|\Phi_{\pm a}\rangle = (|\varphi_{\pm a}\rangle - g|\varphi_{\mp a}\rangle)/\sqrt{1 - 2Sg + g^2}$, where $|\varphi_{\pm a}\rangle$ are the single-particle ground states for the right and left dots, $S = \langle\varphi_{+a}|\varphi_{-a}\rangle$ denotes the overlap integral, and $g = (1 - \sqrt{1 - S^2})/S$. Using $|\Phi_{\pm a}\rangle$, we construct three singlet basis functions with respect to which we diagonalize the two-electron Hamiltonian: Two states with double occupation in each dot, $|RR\rangle = |\Phi_{+a}(z_1)\rangle|\Phi_{+a}(z_2)\rangle$, $|LL\rangle = |\Phi_{-a}(z_1)\rangle|\Phi_{-a}(z_2)\rangle$, and one state with single occupation in each dot, $|LR\rangle = (1/\sqrt{2})[|\Phi_{+a}(z_1)\rangle|\Phi_{-a}(z_2)\rangle + |\Phi_{+a}(z_2)\rangle|\Phi_{-a}(z_1)\rangle]$. Calculating the matrix elements of the Hamiltonian in this orthonormal basis, we obtain

$$H_{HM}(t) = uJ_z^2 + 2wJ_x - \mu(t)J_z, \quad (6)$$

where we have dropped a constant energy term that makes no contribution to the dynamics. In Eq. (6) $u = \langle LL|V_C|LL\rangle - \langle LR|V_C|LR\rangle$ is the difference between the intradot and interdot Coulomb interaction, $w = \langle\Phi_{\pm a}|h(z \mp a)|\Phi_{\mp a}\rangle + \langle LR|V_C|LL\rangle$ denotes the single-particle tunneling induced by dot-dot coupling and the Coulomb interaction, $\mu(t) = 2eF(t)a(1 - g^2)/(1 - 2Sg + g^2)$ describes the electron-field coupling, and J_x and J_z are the x - and z -components of the spin-1 operator. The localized two-particle state $|LL\rangle$ is equivalent to the eigenstate $|j_z = 1\rangle$ of J_z and $|RR\rangle$ to the state $|j_z = -1\rangle$, while the delocalized state $|LR\rangle$ is identical to the state $|j_z = 0\rangle$. According to the expression for u and w , using the material parameters given below Eq. (5) we obtain $u = 12\text{meV}$ and $w = -0.4\text{meV}$.

In the absence of an external driving, the eigenenergies of H_{HM} are $E_1 = (u - \sqrt{u^2 + 16w^2})/2$, $E_2 = u$, and $E_3 = (u + \sqrt{u^2 + 16w^2})/2$, and the corresponding eigenstates are

$$|\varphi_1\rangle = |LL\rangle - E_3/(\sqrt{2}w)|LR\rangle + |RR\rangle, \quad (7a)$$

$$|\varphi_2\rangle = (|RR\rangle - |LL\rangle)/\sqrt{2}, \quad (7b)$$

$$|\varphi_3\rangle = |LL\rangle - E_1/(\sqrt{2}w)|LR\rangle + |RR\rangle. \quad (7c)$$

The symmetric ground state $|\varphi_1\rangle$ is dominated by the delocalized state $|LR\rangle$ due to the strong Coulomb repulsion, whereas the other two eigenstates are nearly degenerate and dominated

by the two localized states $|LL\rangle$ and $|RR\rangle$. The superposition of the two localized states $|LL\rangle$ and $|RR\rangle$ implies that the spatial wave functions of the two electrons have been entangled and correlated, in the usual sense that they cannot be factorized into single-particle states. The nonlinear term in H_{HM} can be exploited to generate entangled states. The ground state of Eq. (7) is plotted in Fig. 2(b). Clearly the HM approximation describes the ground state very well when compared with the exact numerical solution [Fig. 2(a)].

IV. COULOMB-ENHANCED DYNAMIC LOCALIZATION

To investigate dynamic localization, one must start with a localized wave packet. This can be realized from the unperturbed ground state by two separate methods: One is to suddenly switch on a DC field with the strength satisfying the resonance condition $\mu_0 = u$. At time $t \approx \pi/(\sqrt{2}w)$, the delocalized ground state $|\varphi_1\rangle$ evolves into a localized state $|RR\rangle$ with two electrons occupying the same right dot. The alternative method is to adiabatically switch on a constant electric field. Then as shown in Fig. 2(c), the ground state configuration develops a series of Coulomb stairs as a function of the field amplitude, corresponding to a series of avoided crossing in the energy spectrum [see Fig. 2(d)].

After preparing a localized state, say $|RR\rangle$, by adiabatic evolution in the presence of a DC field, the DC field is suddenly switched off and an AC field of the form $F_1 \sin(\omega t)$ is switched on. We show now that the localization can be dynamically maintained by the AC field even when the field strength is small compared to the Coulomb repulsion between the two electrons. Time periodicity of the Hamiltonian enables us to describe the dynamics within the Floquet formalism. In addition, since the Hamiltonian is invariant under the combined dynamic parity operation $z \rightarrow -z$; $t \rightarrow t + \pi/\omega$, each Floquet state is either odd or even. Quasienergies of different parity may cross, otherwise an avoided crossing may occur. Figures 3(a)-(b) show the quasienergy spectra of $H_{HM}(t)$ as a function of F_1 with the presence and absence of the Coulomb interaction, respectively. Two prominent features can be identified from the comparison of these two cases: (i) the strong Coulomb interaction removes the

level crossings among three two-particle states and thus induces avoided crossings; (ii) in the weak field regime, there occurs a crossing between the quasienergies ε_2 and ε_3 , which develop from the unperturbed eigenenergies E_2 and E_3 . To illustrate the effect of this crossing on the system's dynamics, we begin with the initial state $|RR\rangle$ and follow the time evolution of the probability $P_{RR}(t)$ for finding the two electrons in the right dot. The result is shown in Fig. 3(c). It is clear that P_{RR} always remains near 1 as if the two electrons were frozen in the same right dot. This dynamic localization seems counterintuitive at first as the Coulomb repulsion is very strong compared to the AC field, preventing the two electrons occupying the *same* dot. The localization shown in Fig. 3(c) has no correspondence in a non-interacting case, since no level crossings occur in the weak field regime if the Coulomb interaction is absent. Therefore, the present localization effect results from an interplay of the Coulomb interaction and an AC field. Furthermore, we find that even if the Coulomb interaction is strong enough, the dynamic localization can still occur at the crossing of the quasienergies ε_2 and ε_3 . Slightly away from the crossing point, the life time for finding two electrons in the right dot is very long. This makes the experimental realization of the dynamic localization more realistic. The ratio $2\mu_1/\omega$ at the first crossing is about 2.4, a root of the zero-order Bessel function, suggesting that the two-electron localization can be approximated by a two-state model composed of $|\varphi_2\rangle$ and $|\varphi_3\rangle$.

Surprisingly, we find that in the strong field regime, the presence of Coulomb repulsion may help to enhance the dynamic localization when compared with the non-interacting case. From Eq. (7) we see that due to the strong Coulomb interaction, $|RR\rangle \simeq (1/\sqrt{2})(|\varphi_2\rangle + |\varphi_3\rangle)$. Thus the initial localized state can be approximated by a superposition of the degenerate Floquet states developed from the nearly-degenerate states $|\varphi_2\rangle$ and $|\varphi_3\rangle$, which leads to a complete suppression of tunneling at the crossing of the quasienergies ε_2 and ε_3 even in the weak field limit. In the absence of the Coulomb interaction, the initial localized state $|RR\rangle$ is a superposition of all three eigenstates, suggesting dynamic localization at the crossing among three quasienergies. However, the fundamental difference lies in the fact that when the strong interaction is present, the tunneling coupling is $\langle LL|H_{HM}|RR\rangle \simeq 4w^2/u$,

whereas in the absence of the Coulomb interaction the tunneling coupling is $2w$. Thus the coupling between the two localized states greatly decreases in the presence of strong Coulomb interaction, which leads to the enhancement of localization effects.

We emphasize that the localization only occurs at the crossing of the quasienergies developed from the high-energy eigenstates $|\varphi_2\rangle$ and $|\varphi_3\rangle$, in which case the delocalized ground state $|\varphi_1\rangle$ is a dark state during time evolution. For comparison, Figure 3(d) shows $P_{RR}(t)$ with the field parameters corresponding to the crossing of the quasienergies ε_1 and ε_3 . It reveals that dynamic localization disappears and the two electrons start to oscillate between two dots. This fact highlights the essential difference between a single-particle system and an interacting two-particle system. The level crossing of ε_1 and ε_3 induces strong participation of the Floquet state evolved from the unperturbed ground state. As its largest component is the delocalized two-particle state $|LR\rangle$, dynamic localization will be completely destructed, as shown in Fig. 3(d).

V. BELL STATE GENERATION

In this section we investigate the field excitation procedure to obtain a maximally entangled Bell state of the form $|\Psi_{Bell}\rangle = (|RR\rangle + e^{i\phi}|LL\rangle)$ with an arbitrary phase angle ϕ . Figure 4(a) plots the Floquet quasienergies of $H_{HM}(t)$ as a function of the driving frequency ω . It shows that when $\omega = u$, an avoided crossing is formed between the quasienergies ε_1 and ε_2 . Choosing the field parameters at this avoided crossing and starting with the unperturbed ground state, we present in Fig. 4(b) the probabilities $P_{LR}(t)$ for finding the two electrons in different dots, P_{LL} in the left dot, and P_{RR} in the right dot. It shows that the two electrons oscillate between the delocalized state $|LR\rangle$ and two localized states $|LL\rangle$ and $|RR\rangle$. The occupations of two localized states are always the same and the oscillations are always in-phase. Figure 4(c) shows the probability ρ_{Bell} for finding the maximally entangled Bell state with $\phi = \pi$. One can see that ρ_{Bell} varies with time, reaching a maximum value of 1 when $P_{LR} = 0$ (the two electrons are maximally entangled with $\rho_{Bell} = 1$). A direct

numerical solution of Eq. (4) gives the same prediction.

Once the two electrons are in the maximally entangled Bell state, they can remain maximally entangled by suddenly turning off the AC field. We show this effect in Figure 5. Figure 5(a) plots the time evolution of the occupations of three two-particle states, and Figure 5(b) the probability ρ_{Bell} with $\phi = \pi$ (solid line). It is clear from Fig. 5(a) that a pulse of an AC field induces the two electrons to stay in the same dot, while each of them occupies either of the dots with the same probability. As shown in Fig. 5(b) (solid line), the two electrons remain maximally entangled after the electric field is turned off. Therefore, the maximally entangled Bell state can be created and maintained by applying a pulse of a resonant AC field.

We derive an approximate analytical solution to highlight the physical aspect of the Bell-state generation procedure. Taking into account symmetric properties of the three unperturbed eigenstates of the system, the dynamics shown in Fig. 5 is determined by the one-photon transition between the ground state $|\varphi_1\rangle$ and the first excited state $|\varphi_2\rangle$, whereas the transition from $|\varphi_1\rangle$ to $|\varphi_3\rangle$ is prohibited due to their identical symmetry. In this case, we can approximate the Hamiltonian $H_{HM}(t)$ in a Hilbert space spanned by the states $|\varphi_1\rangle$ and $|\varphi_2\rangle$

$$H_{HM}^r(t) = \begin{pmatrix} E_1 & -\sqrt{2}\mu(t)/X \\ -\sqrt{2}\mu(t)/X & E_2 \end{pmatrix}, \quad (8)$$

where $X = \sqrt{4w^2 + E_3^2}/\sqrt{2}w$. In the case of one-photon resonance $E_2 - E_1 = \omega$ and after applying the rotating-wave approximation we obtain the expression for the probability of finding the maximally entangled Bell state

$$\rho_{Bell}(t) = \frac{1}{2}(1 - \cos \phi) \sin^2(w\mu_1 t/u), \quad (9)$$

in the interaction representation and weak coupling limit $u \gg w$. We can see from Eq. (9) that the quantum state of the system at time $\tau = \pi u/(2w\mu_1)$ corresponds to a $\phi = \pi$ maximally entangled Bell state $(|RR\rangle - |LL\rangle)/\sqrt{2}$.

The result of Eq. (9) is shown in Fig. 5(c) (dotted line). Clearly, in comparison with the exact numerical solution (solid line), our two-state approximation describes the system evolution very well. Therefore we arrive at the conclusion that a selective pulse of an AC field with duration $\tau = \pi u / (2w\mu_1)$ can be used to create and maintain a maximally entangled Bell state in the system of two electrons in two coupled quantum dots.

We notice from Eq. (9) that Bell-state generation time is significantly shortened by increasing the amplitude of the AC field. This is important because shorter Bell-state generation time is fundamental to the experimental observation of such maximally entangled state, which is impeded by inevitable decoherence occurred in the realistic double quantum dot system. The decoherence is the most problematic issue pertaining to most quantum computing processing. In the present entangled state proposal, the decohering time depends partly on the fluctuation of the single particle energy caused by the modification of the confining potential due to phononic excitations. There is also a quantum electrodynamic contribution because of coupling to the vacuum modes. In addition, impurity scattering and phonon emission also have contributions to the decoherence. However, in principle, their effects can be minimized by more precise fabrication technology and by cooling the system.

VI. SUMMARY

In summary, we have shown how the dynamic localization and entanglement of two interacting electrons in a coupled quantum dot system can be generated and maintained using an AC field. The Bell-state generation time has been calculated by an analytical approach. Exact numerical calculation confirms these two kinds of Coulomb-involved phenomena. We hope the present study will shed some light on the future development of the coherent control of electrons in quantum dot systems.

ACKNOWLEDGMENT

This work is supported by CNSF under Grant No. 69625608 and by US-DOE.

REFERENCES

- [1] F. Grossmann, T. Dittrich, P. Jung, and P. Hänggi, Phys. Rev. Lett. **67**, 516 (1991).
- [2] R. Bavli and H. Metiu, Phys. Rev. Lett. **69**, 1986 (1992).
- [3] M. Grifoni and P. Hänggi, Phys. Rep. **304**, 229 (1998), and reference therein.
- [4] M. Holthaus and D. Hone, Phys. Rev. B **47**, 6499 (1993).
- [5] T. Zuo, S. Chelkowski, and A.D. Bandrauk, Phys. Rev. A **49**, 3943 (1994).
- [6] F.L. Moore, J.C. Robinson, C.F. Bharucha, Bala Sundaram, and M.G. Raizen, Phys. Rev. Lett. **75**, 4598 (1995).
- [7] D. Loss, and D.P. DiVincenzo, Phys. Rev. A **57**, 120 (1998).
- [8] A. Imamoglu, D.D. Awschalom, G. Burkard, D.P. DiVincenzo, D. Loss, M. Sherwin, and A. Small, Phys. Rev. Lett. **83**, 4204 (1999).
- [9] L. Quiroga and N.F. Johnson, Phys. Rev. Lett. **83**, 2270 (1999).
- [10] E. Biolatti, R.C. Iotti, P. Zanardi, and F. Rossi, Phys. Rev. Lett. **85**, 5647 (2001).
- [11] G. Burkard, G. Seelig, and D. Loss, Phys. Rev. B **62**, 2581 (2000).
- [12] P. Zhang and X.-G. Zhao, Phys. Lett. A **271**, 419 (2000).
- [13] P.I. Tamborenea and H. Metiu, Europhys. Lett. **53**, 776 (2001).
- [14] C.E. Creffield and G. Plattero, Phys. Rev. B **65**, 113304 (2002).
- [15] L. Jacak, P. Hawrylak, and A. Wójs, *Quantum dots* (Springer, Berlin, 1997).
- [16] W.H. Press *et al.*, *Numerical recipes: The Art of Scientific Computing* (Cambridge University Press, Cambridge, England, 1992), 2nd ed.

Figure Captions

FIG. 1. Sketch of two interacting electrons in a coupled quantum dot driven by electric fields.

FIG. 2. (a) Two-electron ground state versus the longitudinal coordinates of the two electrons along diagonal direction $z_1 = -z_2 = z$, obtained via numerically integrating Eq. (4) with no AC field; (b) Two-electron ground state obtained analytically via the Hund-Mulliken approximation; (c) Electron-number distribution of the right dot in the ground state as a function of DC electric field; (d) Low-energy spectrum versus DC field.

FIG. 3. (a) Quasienergy spectrum for two interacting electrons for $\omega = 4.01\text{meV}$; (b) Quasienergy spectrum with no Coulomb interaction; (c) Probability P_{RR} that two electrons occupy the same right dot for an AC field of $F_1 = 1.078\text{kV/cm}$, which produces an exact crossing between two quasienergies that developed from nearly-degenerate two-particle eigenenergies; (d) P_{RR} for $F_1 = 0.76\text{kV/cm}$ and $\omega = 6.4\text{meV}$, corresponding to a crossing between two quasienergies, one of which originates from unperturbed ground-state.

FIG. 4. (a) Floquet spectrum versus the driving frequency of an AC field with a strength $F_1 = 1\text{kV/cm}$; (b) Probabilities that the two electrons are in different combinations of two quantum dots, for a driving frequency $\omega = 12\text{meV}$, corresponding to the avoided crossing shown in (a); (c) Probability ρ_{Bell} as a function of time.

FIG. 5. (a) Probabilities that the two electrons are in different combinations of two quantum dots, with the AC field switched off after $t = 8.1\text{ps}$; (b) Probability ρ_{Bell} as a function of time. The numerical and analytic results are shown with the solid and dotted lines, respectively.

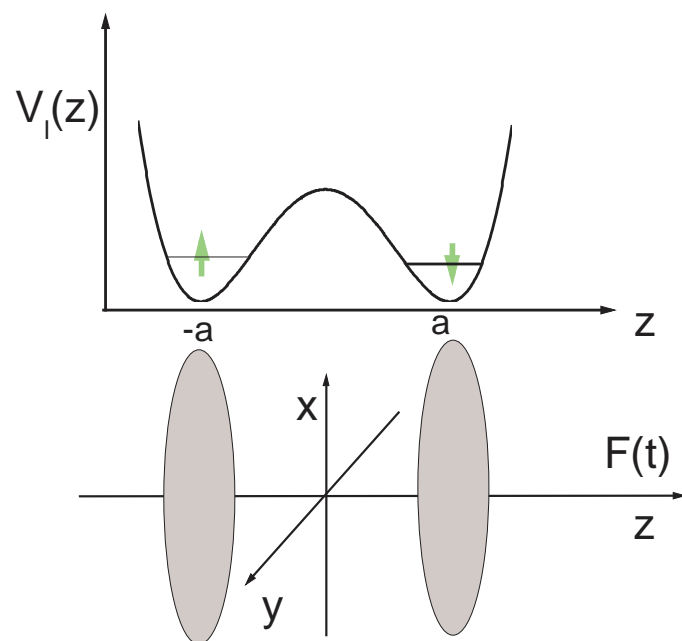


Fig.1

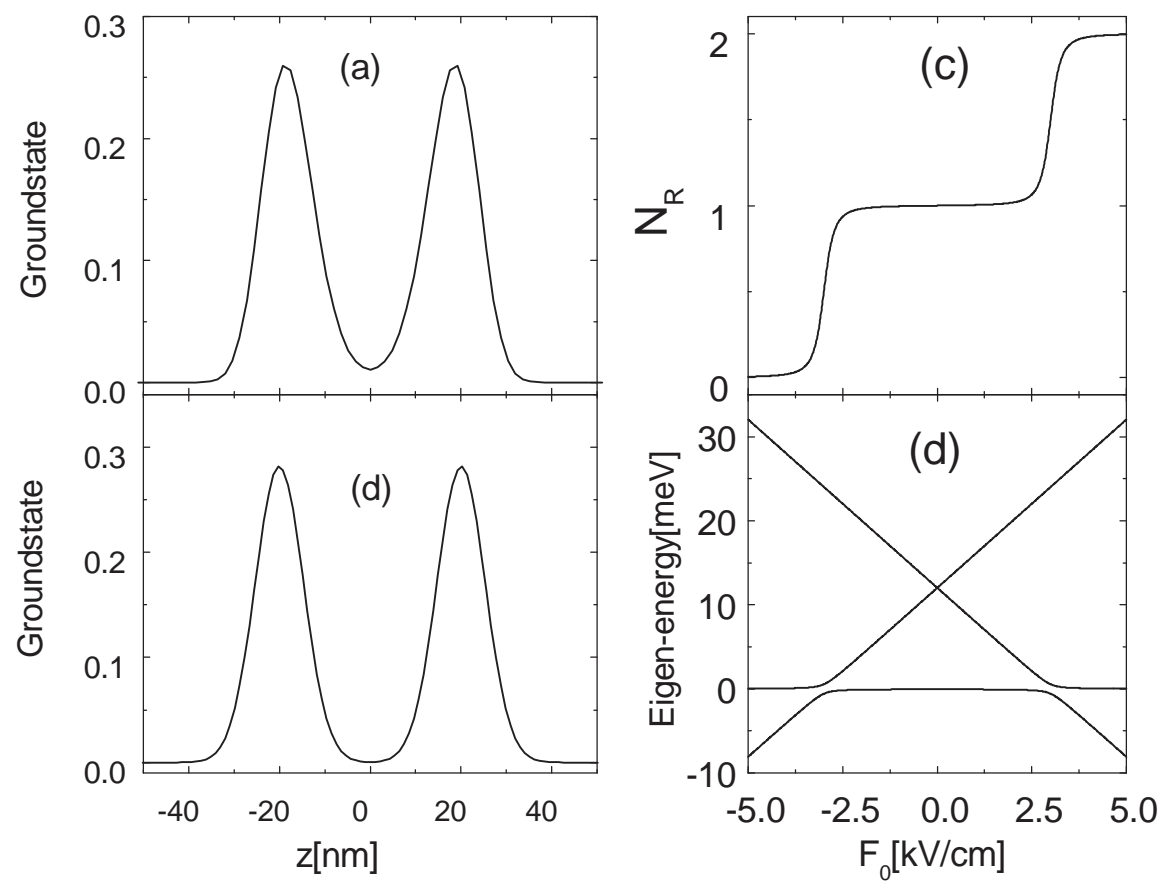


Fig.2

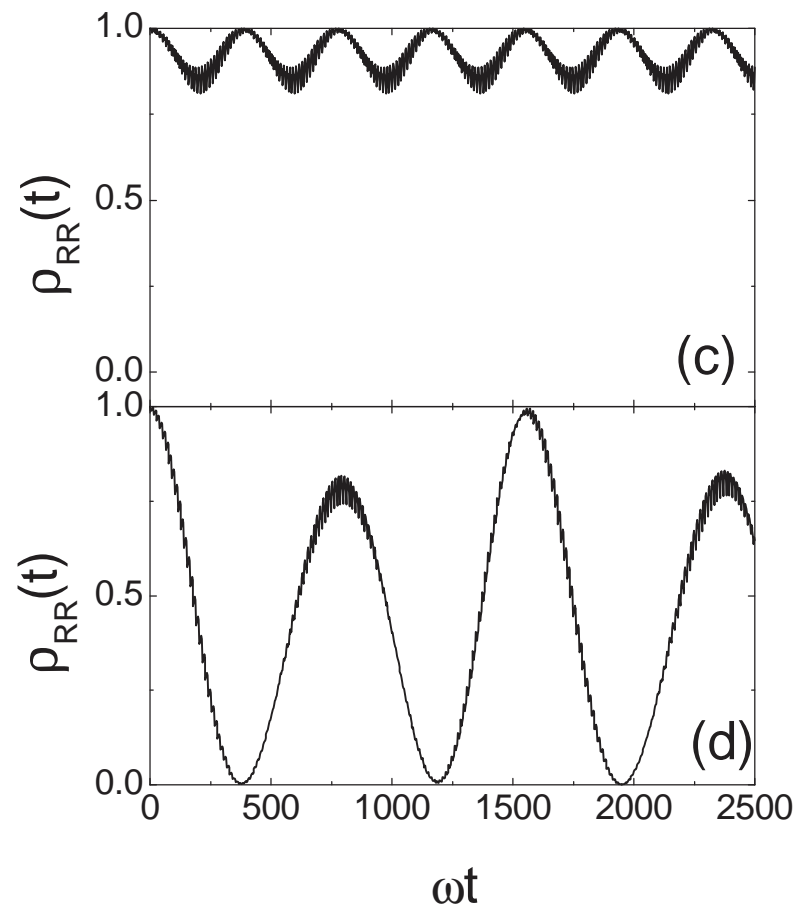
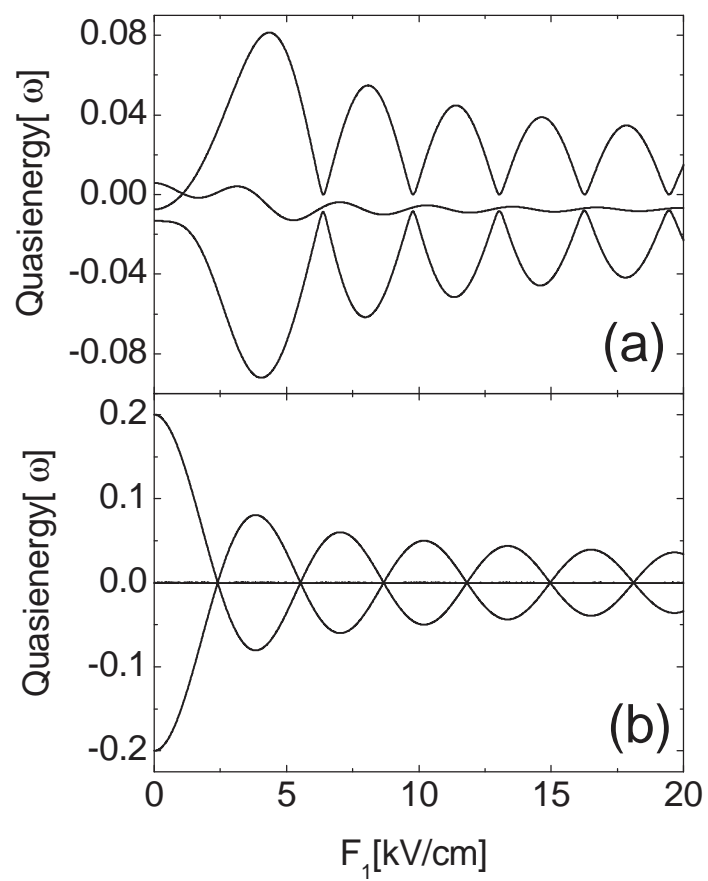


Fig.3

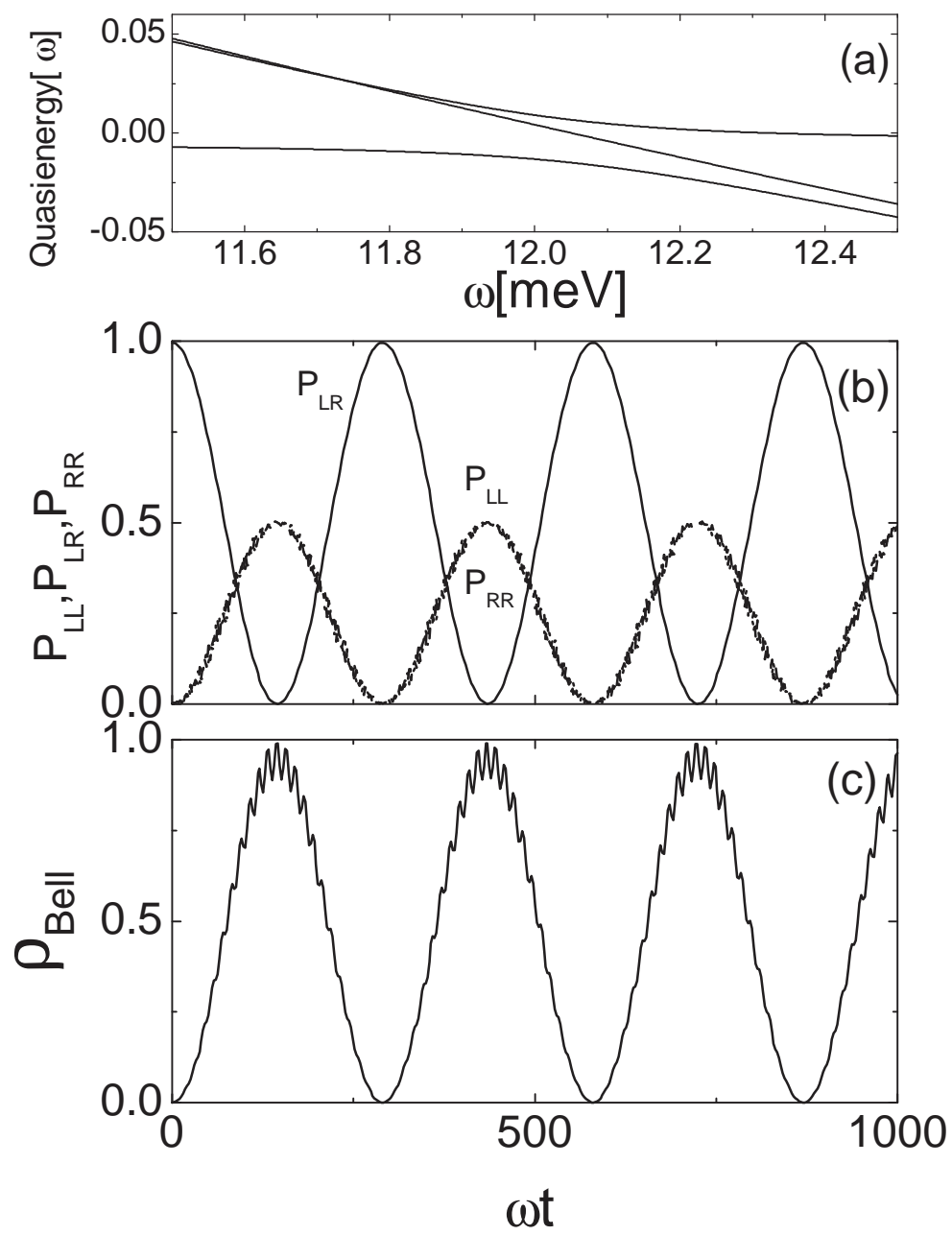


Fig.4

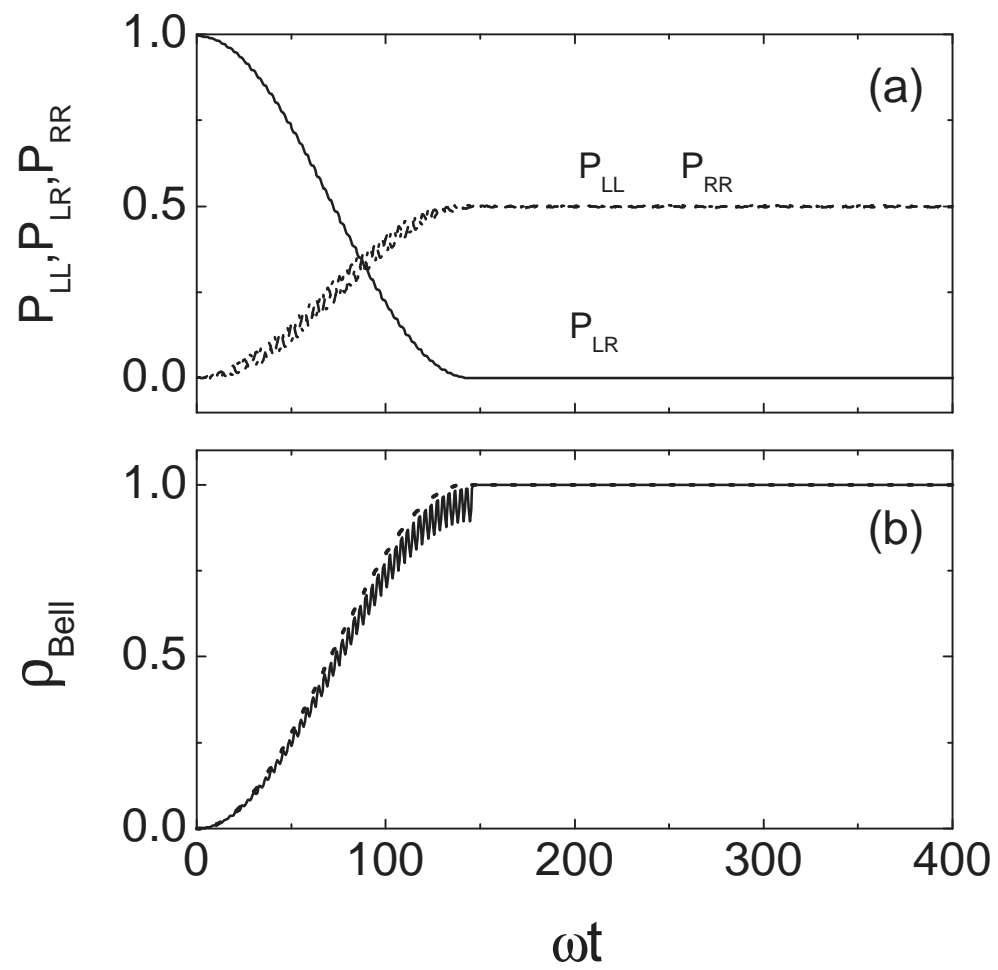


Fig.5